Acta Cryst. (1967). **23**, 1071

Crystal Structure Analysis of AlB_{10} by the Convolution Molecule Method

BY GEORG WILL

Eduard Zintl Institut der Technischen Hochschule, Lehrstuhl für Strukturforschung, Darmstadt, Germany

(*Received* 12 *December* 1966 *and in revised form* 22 *March* 1967)

The crystal structure of AlB_{10} has been solved by analysis of the Patterson projections on (100) and (001) with convolution molecules, and refinement was followed in three dimensions by Fourier and least-squares methods. The structure consists of approximately regular boron icosahedra, linked by direct icosahedral contacts and by intericosahedral boron and aluminum bridges.

Introduction

The higher aluminum borides, AlB_{10} and AlB_{12} and its polymorphs, are distinct from other higher metal borides in that the former combine exact stoichiometric chemical formulae with an anomalous number of formula units per crystallographic unit cell. Despite extended efforts, no crystal structure of any of the higher aluminum borides has thus far been solved. We have therefore undertaken a crystal structure analysis of an AlB_{10} single crystal.

Crystals were obtained by aluminothermic procedures and by a simple melt technique (Kohn, Katz & Giardini, 1958). Michrochemical analysis showed 80·15% B, 19·63% Al, and 79·63% B, 19·32% Al, 0·37% C respectively for the two methods, yielding the chemical formula AlB_{10}. Pycnometric density determinations gave a value of 2·537 g.cm^{-3}; the unit cell is orthorhombic, with $a=8{\cdot}881$, $b=9{\cdot}100$, $c=5{\cdot}690$ Å, yielding 5·2 formula units per unit cell. From the observed extinctions the space group is $B2/b2_1/m2/m$, from which four or eight formula units are to be expected.

From appearance and physical properties (*e.g.* extreme hardness, high melting temperature) it is concluded that the higher aluminum borides are related to elementary boron (Hoard, Hughes & Sands, 1958; Decker & Kasper, 1959; Hughes, Kennard, Sullenger, Weakliem, Sands & Hoard, 1963) and boron carbide, $B_{12}C_3$ (Clark & Hoard, 1943), which crystallize with a close-packed arrangement of boron icosahedra. This concept is also favoured by molecular orbital treatment of the chemical bond between boron atoms (Longuet-Higgins & Roberts, 1955; Lipscomb & Britton, 1960). One would therefore suspect a rigid body framework of icosahedra, or of cube-octahedra or dodecahedra, as the principal building blocks of the crystal structure.

Methods employing rigid units as structure invariant properties were therefore considered most useful for analysis of the structure, and from these the convolution molecule method (Hoppe, 1957) was selected as most promising and easiest to handle in testing an expectedly large number of possible configurations. Also this method had proved very succesful in previous structure determinations (Hoppe & Will, 1960; Will, 1963*a*). Since considerable difficulties had already developed in an attempt to determine the crystal structure of α-AlB_{12} (Eriks, 1961), Fourier transform methods were tried as a parallel second approach. Both methods, convolution molecules as well as Fourier transforms, are rather inconvenient to handle in three-dimensional space, and therefore analysis was started with projections. This offers an additional advantage in reduction in size of the unit cell, and hence of the problem, by a factor of two in (001) (symmetry *gm*) and of four in (100) (symmetry *mm*).

The convolution molecule method

The convolution molecule method aims at the interpretation of a Patterson diagram by comparing the Patterson structure with its individual molecular contributions derived from a suitable model. Convolution molecules are the individual vector sets between the molecules occupying the unit cell of a crystal, and like any Patterson interactions they are expressible by a convolution process. The positions of the convolution molecules in the unit cell are in direct relation to the translation parameters of the molecules, and this general relationship is expressed in the 'convolution diagram', which represents a position diagram for the convolution molecules in the same way that the equivalent positions of a space group describe the positions of the molecules. It is termed a 'convolution diagram' because it derives from a convolution of the set of equivalent positions of the space group with its enantiomorphous set (Will, 1964). Crystal structure analysis with convolution molecules then involves the separation of the structure factor F (summed over the entity of the unit cell) into the molecular contributions of the N individual molecules or, generally, rigid atomic clusters.

$$F=\sum_{j}^{N}\sum_{s_j}^{n_j} f_{s_j,j}\exp[2\pi i(\mathbf{h},\mathbf{x}_j+\mathbf{x}_{s,j})]$$

$$=\sum^{N} F_j\exp[2\pi i(\mathbf{h},\mathbf{x}_j)]\,, \qquad (1)$$

with

$$F_j = \sum_{sj}^{nj} f_{s_j,j} \exp[2\pi i(\mathbf{h}, \mathbf{x}_{s_j,j})]$$

the Fourier transform of the molecule, and

$f_{s_j,j}$ = atomic form factor

N = number of molecules per unit cell

n_j = number of atoms per molecule j

$\mathbf{h}$ = reciprocal lattice vector

$\mathbf{x}_j$ = vector from the origin to the center of the molecule j

$\mathbf{x}_{s_j,j}$ = vectors from the molecular center j to its individual atoms .

Multiplying F with its conjugate complex F^* leads to the Patterson coefficients, which can be split into two parts, $j=j'$ and $j\neq j'$:

$$F \,.\, F^* = \sum_{\substack{j \\ j=j'}}^{N} F_j F_j^* + \sum_{\substack{j \\ j\neq j'}}^{N} \sum_{j'}^{N} F_j F_{j'}^* \exp[2\pi i(\mathbf{h}, \mathbf{x}_j - \mathbf{x}_{j'})] . \quad (2)$$

Fourier transformation of all Patterson coefficients results in the Patterson structure P, with coordinates $\mathbf{x}_p$.

$$P(\mathbf{x}_p) = \sum_h FF^* \exp[2\pi i(\mathbf{h}, \mathbf{x}_p)] = \sum_{\substack{j \\ j=j'}}^{N} \sum_h F_j F_j^* \exp[2\pi i(\mathbf{h}, \mathbf{x}_p)] + \sum_{\substack{j \\ j\neq j'}}^{N} \sum_{j'}^{N} \sum_h F_j F_{j'}^* \exp[2\pi i(\mathbf{h}, \mathbf{x}_j - \mathbf{x}_{j'} + \mathbf{x}_p)] . \quad (3)$$

The first term is zero unless $\mathbf{x}_p = 0$, in which case it is equal to $\sum_j^N \sum_h |F_j|^2$; the second term is zero, unless $\mathbf{x}_p = \mathbf{x}_{j'} - \mathbf{x}_j$. Transformed into direct space the products $F_j F_{j'}^*$ can be replaced by convolutions, and we define convolution molecules as

$$\widehat{\varphi_j \varphi_{j'}^*} = \widehat{\varphi_j \varphi_{j'}^*}(\mathbf{x}_p) = \sum_h F_j F_{j'}^* \exp[2\pi i(\mathbf{h}, \mathbf{x}_p)] \quad (4)$$

where φ_j is the electron density function in direct space describing the molecular model, and $\widehat{\varphi_j \varphi_{j'}^*}$ are derived from that model by convoluting φ_j with $\varphi_{j'}^*$. In practical applications φ_j will be a discontinous function describing a point model of the molecule. For the construction of convolution molecules it has been practical to work with transparent paper on an illuminated lightbox. The two compositions to be convoluted are drawn on two separate sheets; then the origin of sheet one is shifted parallel to every point of the structure on sheet two, and every point of sheet two copied onto sheet one with a weight equal to the product of the two points (Fig. 1).

Equation (4) describes a Patterson function between two molecules j and j' free of translations and depending only on their relative orientation to each other. The Patterson function of the unit cell, equation (3), can therefore be described in terms of N^2 convolution molecules, with N of them located in the origin (for $j=j'$) and $N(N-1)$ at the end of the vectors $(\mathbf{x}_j - \mathbf{x}_{j'})$ (for $j\neq j'$). They are termed equally indexed and mixed indexed convolution molecules respectively:

$$P(\mathbf{x}_p) = \underbrace{\sum_j^N \widehat{\varphi_j \varphi_j^*}(\mathbf{x}_p)}_{\substack{\text{equally indexed} \\ \text{convolution} \\ \text{molecules}}} + \underbrace{\sum_{\substack{j \\ j\neq j'}}^{N} \sum_{j'}^{N} \widehat{\varphi_j \varphi_{j'}^*}(\mathbf{x}_p + \mathbf{x}_j - \mathbf{x}_{j'})}_{\substack{\text{mixed indexed} \\ \text{convolution} \\ \text{molecules}}} . \quad (5)$$

The equally indexed convolution molecules represent the self-Patterson terms and are translation independent located in the origin. In the first step of the analysis they are used to determine the orientations of the molecules. The mixed indexed convolution molecules represent the cross-Patterson terms; they are located in the unit cell at the end of vectors $(\mathbf{x}_j - \mathbf{x}_{j'})$ and lead to the determination of the translation parameters $\mathbf{x}_j$ of the molecules. This approach allows a complete and straightforward interpretation of a Patterson calculation provided a molecular model is sufficiently well known.

Two-dimensional analysis

Two-dimensional data were collected on a precession camera with $\mu = 30°$ using Mo $K\alpha$ radiation. The intensities were estimated visually. With 5·2 formula units of AlB_{10} per unit cell we conclude that four boron icosahedra (48 borons atoms) plus four linking boron atoms form the main structure. In (100) with only one-fourth of the unit cell, the one B_{12} unit is expected to dominate the Patterson projection. Further there is only one convolution molecule, which is the vector set of the icosahedron itself (Fig. 1); it is centred in the origin with only freedom of rotation around the three axis.

With a total of four icosahedra in the unit cell, their centres must be located in the point positions 4(*a*), or 4(*b*), or 4(*c*) of space group *Bbmm*. The point symmetries are 2/*m*, 2/*m*, and *mm* respectively, and this restricts the orientation of the icosahedra to only a few possibilities. If it is further assumed, as is justified by analysis in (001), that the icosahedra are centred in 4(*c*), *i.e.* outside the origin or face centres, there are only two orientations left in (100), and these differ by rotation of 90° of the model shown in projection in Fig. 1. The vector set, or convolution molecule, of an icosahedron (Fig. 1) has been superimposed with these two orientations on the Patterson projection $P(vw)$, and agreement between model and observed vector distribution is found only for the x axis of the icosahedron along [010] (Fig. 2). Similar tests with other orientations and also with cube-octahedra and dodecahedra failed

to show any satisfactory agreement with the observed Patterson structure.

The Fourier transforms of these models were also calculated and compared with the observed, weighted reciprocal lattice. Fig. 3 depicts some typical examples of these tests, and again the best agreement is found for an icosahedron in projection as shown in model **b** of Fig. 3 with the icosahedral x axis parallel to [010] [Fig. 3(*a*)]. Since we are considering only the boron icosahedron, which represents only 83% of the content of the unit cell, the agreement is not quite as perfect as usually. The main features however are given correctly only in the orientation of Fig. 3(*a*) with large discrepancies in other orientations and models. Comparing Fig. 3(*a*) and 3(*b*), for example, we find $F(022)$, the strongest reflexion in Fig. 3(*b*), in a field of almost

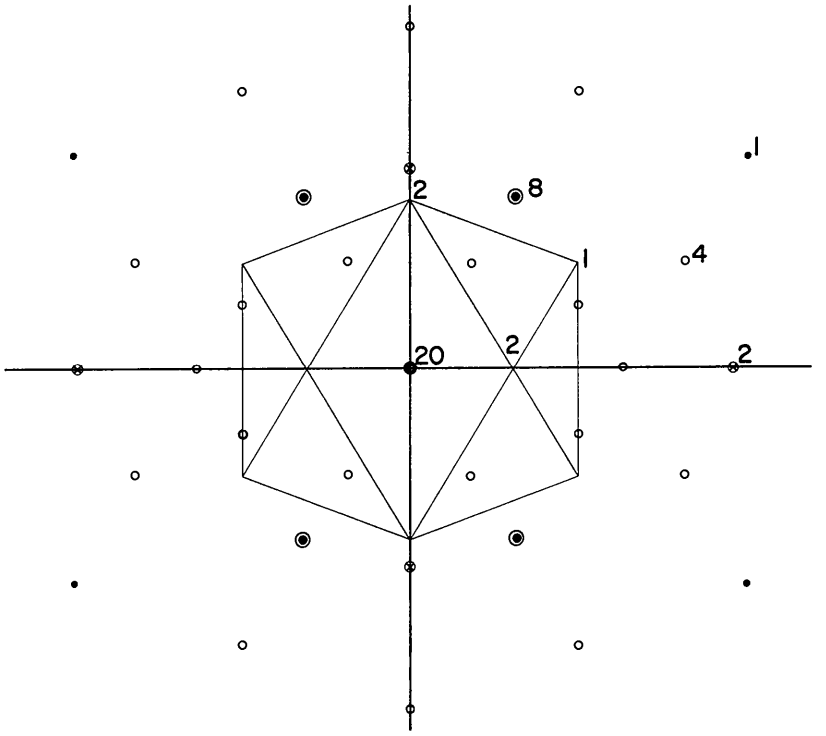

Fig. 1. Convolution molecule $\widehat{\varphi_1\varphi_1}^*$ of an icosahedron in projection.

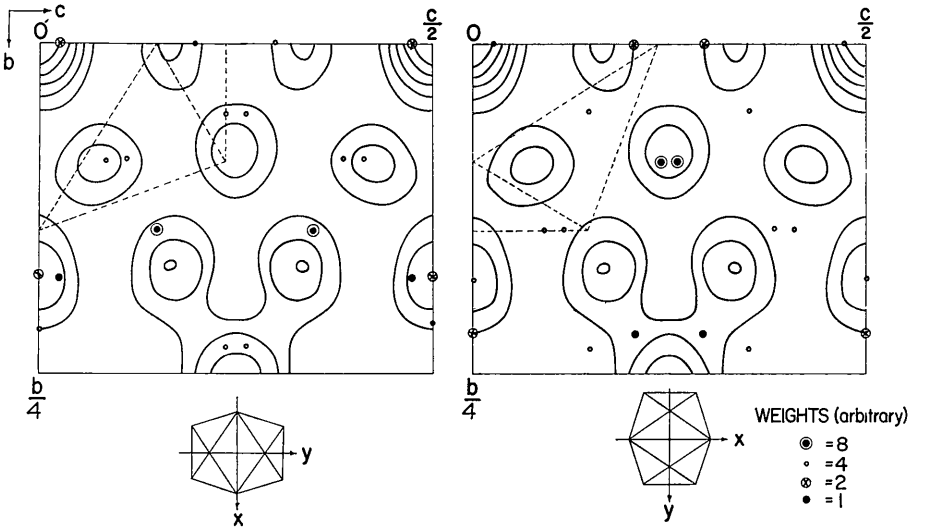

Fig. 2. Patterson projections $P(vw)$ with convolution molecule $\widehat{\varphi_1\varphi_1}^*$ superimposed at two possible orientations. $\widehat{\varphi_1\varphi_1}^*$ is centred in the origin. (The unit cells in Figs. 2, 4 and 5 are distorted owing to computer output of the diagrams).

zero density. $F(042)$, on the other hand, is expected to be rather strong from Fig. 3(*b*), while it should be weak from Fig. 3(*a*). The observed value of $F(042)$ is zero. A similar situation is found for $F(082)$ and $F(0,10,4)$. As a final test $|F|^2$ values were taken from the Fourier transform map at the properly oriented reciprocal lattice of Fig. 3(*a*) and a Fourier series was calculated. The ensuing diagram (Fig. 4) is nearly identical with the observed Patterson projection $P(vw)$.

In (001), with the unit cell reduced to one half of its size, two icosahedra are expected and hence four convolution molecules, two in the origin and two outside the origin. Also in (001) Al–Al (and Al–B) interaction vectors should show up in the Patterson projection, and in the first examination of $P(uv)$ (Fig. 5), the peak at $u=0{\cdot}2a$, $v=0{\cdot}5b$, with half the weight of the origin peak was considered an Al–Al vector. In the ensuing calculations, Al was expected to act as a heavy atom in phasing the structure factors, but no indications of structural features related to icosahedra were seen.

Analysis with convolution molecules was then renewed. If the two icosahedra are designated φ_1 and φ_2, four convolution molecules $\widehat{\varphi_j\varphi_{j'}^*}$, $(j,j'=1,2)$ are obtained at positions listed in Table 1, which are derived from the equivalent positions 4(*c*) at $\pm(x,\frac{1}{4},0)$.

In general, mixed indexed convolution molecules, located outside the origin, have a fairly random distribution of peaks, in contrast to equally indexed convolution molecules centred in the origin, which always have the high origin maximum of the self-Patterson (see Fig. 1). When the molecules exhibit symmetry properties, however, ordering of the peaks takes place, and in a benzene configuration, for example, the sixfold symmetry shows up. The highest degree of ordering possible is found when symmetry elements in the molecule, for example mirror planes, become oriented

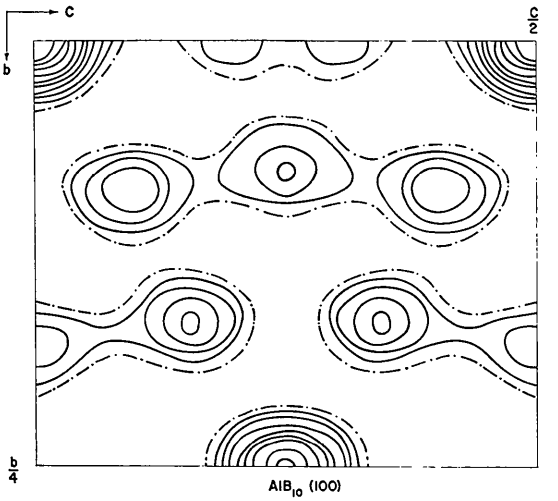

Fig. 4. Patterson projection $P(vw)$ of an icosahedron model calculated with $|F|^2$ values taken from the Fourier transform of Fig. 3. To be compared with Fig. 2.

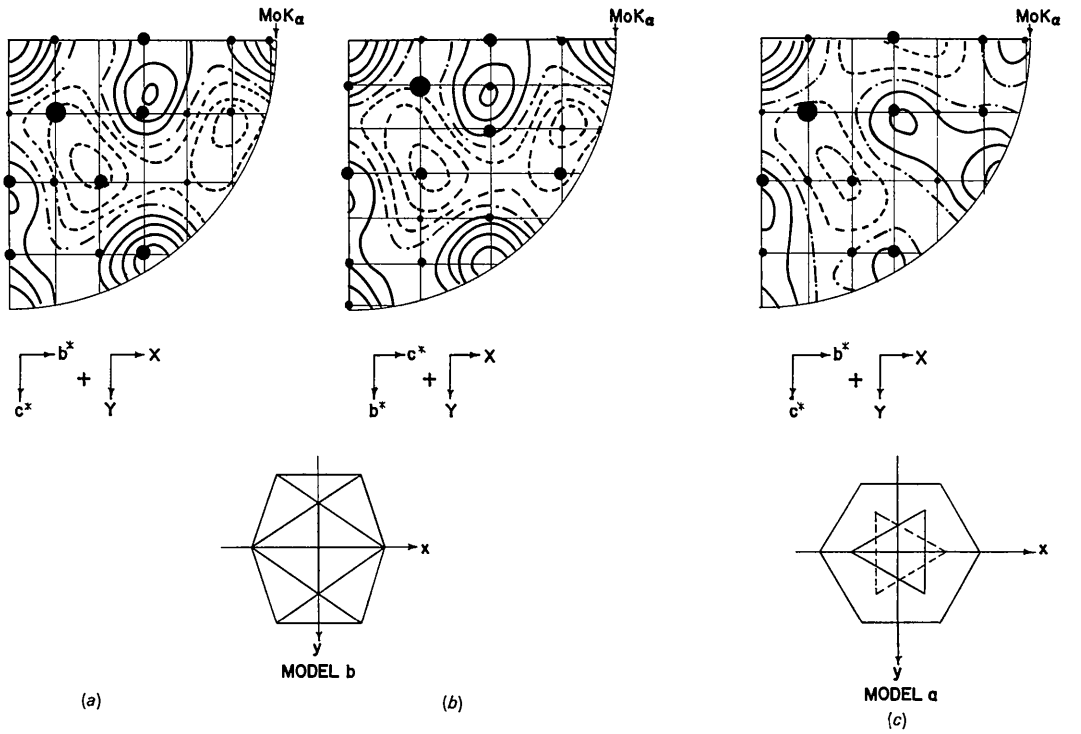

Fig. 3. Observed weighted reciprocal lattice (100) superimposed on the Fourier transform of an icosahedron at different orientations, Mo $K\alpha$ indicates the region in reciprocal space observable on a precession camera with $\mu=30°$.

Table 1. *Positions of convolution molecules in projection* (001) *of space group Bbmm*

Convolution molecule	x/a	y/b	
$\widehat{\varphi_1\varphi_1}^*$, $\widehat{\varphi_2\varphi_2}^*$	0	0	Equally indexed $j=j'$
$\widehat{\varphi_1\varphi_2}^*$	$2x$	$\frac{1}{2}$	Mixed indexed $j\neq j'$
$\widehat{\varphi_2\varphi_1}^*$	$-2x$	$\frac{1}{2}$	

parallel to identical symmetry elements in the unit cell. In this case, complete ordering of the maxima in the convolution molecule takes place in such a way that the mixed indexed convolution molecules become identical with the equally indexed convolution molecules (Will, 1963*a*). Since every equally indexed convolution molecule exhibits the high central Patterson maximum, this same maximum will now also be found outside the origin at $2\mathbf{x}_p$. From Table 1 it can be seen, that, in projection (001) in space group *Bbmm*, there will be two such maxima at $\pm(2x,\frac{1}{2}b)$ with weight one half of the origin peak; this is in agreement with observation. Consequent superposition of the four convolution molecules on the Patterson projection $P(uv)$ resulted in complete agreement with the observed vector distribution (Fig. 5).

These considerations then determine the coordinates for the two icosahedral centres together with the orientation of the icosahedra and allow the placement of 48 boron atoms out of a total of 52. (The projection (001) allows for two possible parameter values due to the symmetry in Patterson space; $\frac{1}{2}(0{\cdot}2a,0{\cdot}5b)$ and $\frac{1}{2}[(\frac{1}{2}-0{\cdot}2)a,0{\cdot}5b]$, and the latter was uniquely determined by the three-dimensional analysis). Structure factor calculations in projections with this model resulted in an R value of 29%, and the ensuing Fourier syntheses showed the icosahedra together with two additional peaks, at which boron atoms were placed. Least-squares calculations, using the combined (001) and (100) data, then decreased R to 20·4% (Will, 1963*b*).

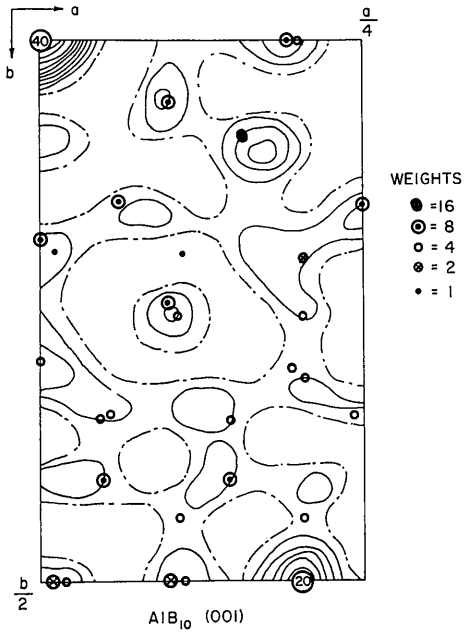

Fig. 5. Patterson projection $P(uv)$ with four convolution molecules $\widehat{\varphi_j\varphi_{j'}}^*(j,j'=1,2)$ superimposed.

Up to this point, aluminum atoms, which should show up in a Fourier map of boron atoms with considerable intensity, were not seen. It was assumed therefore, that Al was statistically distributed over several sites, which is consistent also with the complete absence of any Al–Al interaction vectors in the Patterson projections, and the structure analysis was therefore extended to three dimensions.

Three-dimensional analysis

Three-dimensional data were collected by Weissenberg multiple film technique from the zero to 5th layers, rotating the crystal around [010] and using Cu $K\alpha$ radiation. To assure accuracy necessary for locating statistically distributed atoms the films were processed in temperature controlled baths, and densities were measured with a Joyce–Loebl flying-spot integrating densitometer. The reproducibility of the density measurements is better than 1%, and the standard deviations of the intensities calculated from equivalent reflexions measured on films of different exposure were about 3 to 10%.

With the approximate parameters from the two-dimensional model as starting values, three-dimensional Fourier and difference Fourier maps were calculated, revealing several additional peaks. These sites were subsequently occupied by aluminum and the occupancy figure was then allowed to vary in the ensuing least-squares calculations. Atoms Al(1) to Al(4) were thus located in several cycles of difference Fourier and least-squares calculation, and a final error index $R=\Sigma\,||F_o|-|F_c||/\Sigma\,|F_o|$ of 0·079 was reached, excluding the non-observed reflexions. The square root sum $\Sigma w\,.\,\Delta F^2/(n_0-n_v)$ was 1·06. For the refinement non-observed reflexions were given about half the minimum observable values, and strong reflexions suspected of being affected by extinction were weighted zero. The weighting scheme was $\sigma\propto|/F$, which we found most satisfying considering the method used for data collection, where all but the very weak reflexions are measured with about equal accuracy on the linear part of the film density curve. The final parameters are listed in Table 2 .

Discussion

The crystal structure of AlB_{10} consists of four nearly regular boron icosahedra of symmetry *mm*, centred in the positions 4(*c*) of space group *Bbmm*, $\pm(x,\frac{1}{4},0)$ and $\pm(\frac{1}{2}+x,\frac{1}{4},\frac{1}{2})$, with $x=0{\cdot}152$. The B–B bond lengths

Table 2. *Atomic coordinates and their standard deviations, isotropic temperature coefficients and occupancy figures*

	Equivalent position and occupancy number		x/a	$\sigma(x)$ $\times 10^5$	y/b	$\sigma(y)$ $\times 10^5$	z/c	$\sigma(z)$ $\times 10^5$	B
B(1)	8(*f*)	8·0	0·04752	50	0·08607	76	0·0		0·26
B(2)	8(*f*)	8·0	0·25157	48	0·09053	72	0·0		0·13
B(3)	16(*h*)	16·0	0·15211	31	0·15288	77	0·25338	58	0·25
B(4)	8(*g*)	8·0	0·31975	50	0·25		0·15816	80	0·26
B(5)	8(*g*)	8·0	0·48400	49	0·25		0·33916	81	0·26
B(*b*)	8(*f*)	4·0	0·15257	52	0·06191	131	0·5		0·81
Al(*b*)	8(*f*)	1·83							
Al(1)	4(*c*)	0·75	0·28883	117	0·25		0·5		0·56
Al(2)	4(*b*)	1·06	0·0		0·0		0·5		0·92
Al(3)	16(*h*)	1·02	0·46098	121	0·04875	287	0·17472	217	0·10
Al(4)	8(*f*)	0·24	0·34449	611	0·12999	1529	0·5		0·1

Table 3. *Comparison between the observed and calculated structure factors*

H K L	F(OBS)	F(CALC)	H K L	F(OBS)	F(CALC)	H K L	F(OBS)	F(CALC)
2 0 0	14.4	-13.5	3 1 5	3.7	2.8	2 3 4	19.6	-21.4
4 0 0	8.3	8.8	5 1 5	16.4	-15.6	4 3 4	3.3	-2.6
6 0 0	51.4	56.1	7 1 5	3.3	2.8	6 3 4	3.0	1.1
8 0 0	9.0	9.9	2 1 6	22.5	22.5	8 3 4	14.4	-13.5
10 0 0	41.7	-43.2	4 1 6	20.0	-20.9	1 3 5	7.4	-6.4
1 0 1	0.0	4.4	6 1 6	3.4	2.6	3 3 5	4.5	4.9
3 0 1	47.9	46.2	1 1 7	7.7	-9.5	5 3 5	38.6	-41.2
5 0 1	3.4	-4.6	3 1 7	3.5	3.9	7 3 5	4.3	3.4
7 0 1	22.5	-24.6	2 2 0	13.0	13.3	2 3 6	20.3	-19.4
9 0 1	6.5	5.4	4 2 0	2.4	3.5	4 3 6	4.8	3.8
11 0 1	11.2	-10.1	6 2 0	22.5	-19.8	2 4 0	24.8	24.9
0 0 2	28.3	21.8	8 2 0	10.4	8.9	4 4 0	25.8	28.5
0 0 4	65.4	67.1	10 2 0	21.5	-20.9	6 4 0	19.2	23.7
2 0 2	4.9	-4.1	1 2 1	23.7	-24.7	8 4 0	9.0	-6.6
4 0 2	34.8	33.5	3 2 1	5.1	-4.7	10 4 0	38.3	41.5
6 0 2	28.2	-27.5	5 2 1	12.9	-15.8	1 4 1	14.1	-13.6
8 0 2	6.6	7.1	7 2 1	18.2	-19.8	3 4 1	3.5	-2.5
10 0 2	7.1	-7.1	9 2 1	14.1	-13.8	5 4 1	5.0	-2.6
1 0 3	6.0	-2.8	0 2 2	61.5	67.3	7 4 1	0.0	-2.8
3 0 3	9.8	-7.8	2 2 2	2.5	2.7	9 4 1	13.7	13.4
5 0 3	0.0	-1.3	4 2 2	4.8	-2.8	0 4 2	3.2	3.1
7 0 3	33.7	-35.6	6 2 2	24.5	26.8	2 4 2	7.4	-6.8
9 0 3	22.4	-22.6	8 2 2	11.7	10.9	4 4 2	25.8	-23.9
0 0 4	65.4	67.1	10 2 2	15.8	-16.6	6 4 2	21.6	21.8
2 0 4	19.4	-20.3	1 2 3	5.8	4.5	8 4 2	7.7	5.1
4 0 4	12.6	-13.5	3 2 3	45.7	47.3	1 4 3	28.7	-29.5
6 0 4	10.3	9.6	5 2 3	9.4	-8.6	3 4 3	32.6	-35.3
8 0 4	15.3	15.2	7 2 3	4.5	-4.1	5 4 3	4.5	-2.2
1 0 5	4.8	-4.4	9 2 3	7.4	6.1	7 4 3	17.9	-17.1
3 0 5	20.4	18.6	0 2 4	30.4	33.1	9 4 3	8.8	-8.4
5 0 5	3.4	-2.5	2 2 4	11.5	9.7	0 4 4	37.2	-42.1
7 0 5	29.8	-18.8	4 2 4	16.4	13.7	2 4 4	9.1	8.2
0 0 6	47.7	48.6	6 2 4	13.4	13.8	4 4 4	7.1	5.7
2 0 6	10.5	10.5	8 2 4	6.3	6.3	6 4 4	15.5	-14.0
4 0 6	36.6	38.2	1 2 5	13.7	-13.0	1 5 5	9.6	-8.6
6 0 6	1.7	-0.7	3 2 5	0.0	0.7	3 5 5	6.1	-6.3
1 0 7	6.4	5.9	5 2 5	10.2	-10.2	5 5 5	0.0	-3.8
2 1 0	30.9	-30.6	7 2 5	13.0	-11.5	7 5 5	0.0	-3.3
4 1 0	2.9	1.1	0 2 6	11.4	10.4	0 6 6	39.9	31.9
6 1 0	29.5	31.3	2 2 6	0.0	1.2	2 6 6	3.8	3.3
8 1 0	17.8	-18.0	4 2 6	10.2	-8.3	4 6 6	8.4	-7.4
10 1 0	4.0	4.6	6 2 6	4.1	-5.7	2 5 0	27.8	28.5
1 1 1	14.7	-14.6	1 2 7	9.6	-8.5	4 5 0	18.5	-17.6
3 1 1	8.9	6.5	2 3 0	61.3	-64.2	6 5 0	13.4	13.8
5 1 1	17.9	-15.7	4 3 0	22.8	21.7	8 5 0	21.1	23.1
7 1 1	0.0	1.5	6 3 0	15.6	-14.2	10 5 0	2.9	2.4
9 1 1	0.0	1.5	8 3 0	31.0	-31.4	1 5 1	6.5	5.6
11 1 1	8.3	9.6	10 3 0	6.3	3.4	3 5 1	4.5	1.8
2 1 2	11.7	11.9	1 3 1	4.4	-5.1	5 5 1	16.7	-17.5
4 1 2	22.9	-22.4	3 3 1	6.9	6.6	7 5 1	3.0	-3.5
6 1 2	17.6	-17.2	5 3 1	51.4	-59.6	9 5 1	7.8	6.2
8 1 2	0.0	-0.1	7 3 1	7.5	7.6	2 5 2	46.3	-52.6
10 1 2	0.0	-0.5	9 3 1	18.2	-16.2	4 5 2	17.7	17.4
1 1 3	15.1	13.9	2 3 2	18.1	-17.2	6 5 2	10.1	9.7
3 1 3	7.5	-6.8	4 3 2	11.6	-10.2	8 5 2	39.9	-46.6
5 1 3	27.4	-29.9	6 3 2	12.9	-10.0	1 5 3	23.0	25.2
7 1 3	9.6	9.7	8 3 2	7.8	-8.0	3 5 3	3.7	-1.8
9 1 3	22.8	-21.8	10 3 2	3.7	-3.2	5 5 3	28.3	-27.9
2 1 4	35.5	-36.9	1 3 3	20.7	-20.2	7 5 3	13.8	13.7
4 1 4	11.6	11.1	3 3 3	22.9	23.8	9 5 3	18.4	-18.1
6 1 4	1.9	2.8	5 3 3	22.1	-23.2	2 5 4	0.0	-0.5
8 1 4	34.1	-35.2	7 3 3	7.1	7.2	4 5 4	11.1	-10.4
1 1 5	0.0	-0.4	9 3 3	11.8	11.7			

within the icosahedra (Table 4) are in close agreement with values reported previously for compounds containing boron icosahedra, like tetragonal boron (Hoard *et al.*, 1958). The mean value for the edge of the icosahedra in AlB_{10} is $1{\cdot}810 \pm 0{\cdot}003$ Å, which compares very well with $1{\cdot}805 \pm 0{\cdot}015$ Å observed in tetragonal boron. The angles of the triangles of the icosahedra (Table 5) are very close to the ideal value of 60°, with an average value of $59{\cdot}84° \pm 0{\cdot}16°$. The regularity of the icosahedra makes substitution of aluminum for boron within the icosahedra unlikely, a view brought forward to explain the unreasonable number of 5·2 formula weights in the unit cell (Lipscomb & Britton, 1960). The difference of radii of B and of Al would require distortion in contrast with the observed structure.

The structure can be looked upon as consisting of closed-shell type boron icosahedra, as treated by Longuet-Higgins & Roberts (1955). The 48 atomic orbitals of one icosahedron are combined into 13 bonding and 17 antibonding molecular orbitals, which lie within the

Table 4. *Interatomic distances*

(*a*) Bond lengths within the icosahedron. (The numbers of bonds per icosahedron are given in parentheses).

B(1)–B(2)	(2)	$1{\cdot}812 \pm 0{\cdot}006$ Å
B(1)–B(3)	(4)	$1{\cdot}820 \pm 0{\cdot}005$
B(1)–B(5)	(4)	$1{\cdot}839 \pm 0{\cdot}006$
B(2)–B(3)	(4)	$1{\cdot}783 \pm 0{\cdot}005$
B(2)–B(4)	(4)	$1{\cdot}812 \pm 0{\cdot}006$
B(3)–B(3)	(2)	$1{\cdot}768 \pm 0{\cdot}010$
B(3)–B(4)	(4)	$1{\cdot}814 \pm 0{\cdot}006$
B(3)–B(5)	(4)	$1{\cdot}813 \pm 0{\cdot}006$
B(4)–B(4)	(1)	$1{\cdot}800 \pm 0{\cdot}006$
B(5)–B(5)	(1)	$1{\cdot}830 \pm 0{\cdot}006$
B–B average		$1{\cdot}810 \pm 0{\cdot}003$

(*b*) External bonds between icosahedra

B(4)–B(5)	(4)	$1{\cdot}786 \pm 0{\cdot}006$ Å
B(1)–B(1)	(2)	$1{\cdot}779 \pm 0{\cdot}009$
B(b)–B(2)	(2)	$1{\cdot}628 \pm 0{\cdot}012$
B(b)–B(3)	(4)	$1{\cdot}629 \pm 0{\cdot}007$

(*c*) Interatomic distances of inter-icosahedral atoms

B(b)–Al(1)		$2{\cdot}096 \pm 0{\cdot}012$ Å	
B(b)–Al(2)		$1{\cdot}467 \pm 0{\cdot}007$	
B(b)–Al(3)		$1{\cdot}974 \pm 0{\cdot}012$	$1{\cdot}738 \pm 0{\cdot}019$ Å
B(b)–Al(4)		$1{\cdot}813 \pm 0{\cdot}070$	
Al(1)–B(3)	(4)	$2{\cdot}055 \pm 0{\cdot}007$	
Al(1)–B(4)	(2)	$1{\cdot}964 \pm 0{\cdot}005$	
Al(1)–B(5)	(2)	$1{\cdot}960 \pm 0{\cdot}010$	
Al(1)–Al(4)		$1{\cdot}199 \pm 0{\cdot}129$	
Al(3)–B(1)		$2{\cdot}033 \pm 0{\cdot}013$	
Al(3)–B(3)		$1{\cdot}986 \pm 0{\cdot}020$	
Al(3)–B(5)		$2{\cdot}067 \pm 0{\cdot}024$	
Al(3)–Al(2)		$1{\cdot}142 \pm 0{\cdot}015$	
Al(3)–Al(3)		$1{\cdot}126 \pm 0{\cdot}031$	$1{\cdot}988 \pm 0{\cdot}017$
Al(4)–B(1)		$1{\cdot}847 \pm 0{\cdot}061$	
Al(4)–B(5)		$1{\cdot}888 \pm 0{\cdot}088$	

icosahedra, and 12 orbitals with *sp* hybrids pointing outward perpendicular to the icosahedra. To fill the orbitals 38 electrons are required. The 12 icosahedral boron atoms can contribute only 36 electrons, so two additional electrons have to be transfered to each boron

Table 5. *Main bond angles in the boron isocahedron*

The errors are approximately 0·2°.

Atom designation	Bond angle	Atom designation	Bond angle
2–1–3 (*a*)*	58·82°	3–1–5 (*a*)	106·25°
5–1–5′ (*a*)*	59·70	2–1–5 (*a*)	106·77
3–1–5	59·41	3–1–3′	104·81
1–2–3 (*a*)	60·79	1–2–4 (*a*)	110·61
4–2–4′ (*a*)	59·57	3–2–3′ (*a*)	107·88
3–2–4	60·60	3–2–4	108·19
1–3–2	60·39	1–3–3	109·52
1–3–5	60·82	1–3–4	110·18
2–3–4	60·47	2–3–3	108·55
3–3–4	60·84	2–3–5	109·15
3–3–5	60·82	4–3–5	110·58
2–4–3 (*a*)	58·93	2–4–3′ (*a*)	105·33
2–4–4 (*a*)	60·22	3–4–4 (*a*)	107·38
3–4–3′	58·31	2–4–2′	106·45
1–5–3 (*a*)	59·77	1–5–3′ (*a*)	106·71
1–5–5 (*a*)	60·15	3–5–5 (*a*)	106·88
3–5–3′	58·35	1–5–1′	108·44

* (*a*) denotes two equivalent angles of this type per icosahedron. Primed figures distinguish equivalent positions of boron atoms.

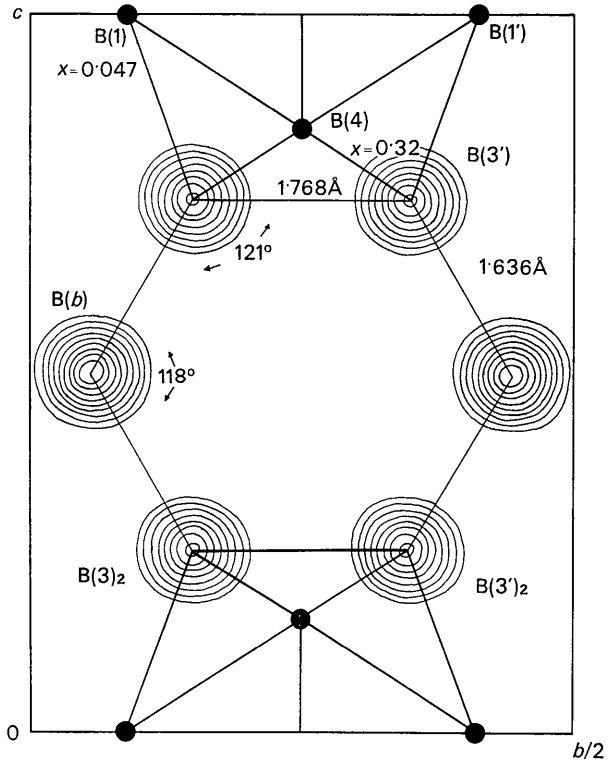

Fig. 6. Section of Fourier map at $x=0{\cdot}152a$ depicting connexion of two icosahedra in (100) planes along [001] through bridges B(*b*) occupied statistically by boron (50 %) and aluminum (23 %). The site B(*b*) is not completely filled. Atoms B(1) and B(4) are outside the given Fourier section.

icosahedron from intericosahedral sources, and some of the aluminum atoms seem to be required in addition to the borons.

Of the twelve boron atoms of each icosahedron six have bonds to neighbouring icosahedra in the direction of the *sp* hybrids: B(1)–B(1′) = 1·779 Å, and B(4)–B(5′) = B(5)–B(4′) = 1·786 Å, while B(2) and B(3) must be bonded through *sp* hybrids by way of bridges over additional boron and aluminum atoms. For such connexions we find two sites, 4(*c*) and 8(*f*). 4(*c*), with $x=0{\cdot}79$, has eightfold coordination to boron atoms B(3), B(4) and B(5) of three icosahedra at distances 2·01 Å. Bonds from 4(*c*) to icosahedral boron atoms, however, would require considerable bending of the *sp*-hybrid orbitals from their direction normal to the icosahedra and these atoms probably only fill holes in the relatively open framework of the close-packed icosahedra. 8(*f*) is at distances of 1·63 Å to boron atoms B(2), B(3) and B(3′) of three icosahedra with the *sp* hybrids pointing approximately to the atoms at these sites, and we conclude that 8(*f*) serves as a bridge between neighbouring icosahedra by way of *sp*-hybrid bonds. The direct icosahedral contacts B(1)–B(1′) are found in (001) planes, and the B(4)–B(5′) bonds in (010) planes, while atoms B(*b*) in 8(*f*) form strong connexions between icosahedra in (100) planes. Icosahedra are linked through two B(*b*) bridges to the next icosahedra forming chains of icosahedra along [001]. It is of interest to note the almost regular boron hexagon of the $B(3)_1$–$B(3')_1$–B(*b*)–$B(3)_2$–$B(3')_2$–B(*b*′) bond system (Fig. 6) of two icosahedra 1 and 2 (subscript). The B(*b*) atoms also establish additional connexions [besides B(1)–B(1′) and B(4)–B(5′)] of the chains of icosahedra by forming bonds to atoms B(2) of a third icosahedron.

In distributing atoms properly over 4(*c*) and 8(*f*) there is, however, some ambiguity. After placing 48 borons in icosahedra, we have only four more boron atoms per unit cell left, and one would suggest occupying 4(*c*) with boron atoms and 8(*f*) with aluminum atoms. This, however, results in aluminum bridges between icosahedra, which has not been observed so far. Refinement of this model stopped at an *R* value of 9·6%, and led to 2·7 boron atoms in 4(*c*), and 2·7 aluminum atoms in 8(*f*). Another choice is to occupy 8(*f*) statistically with four boron *and* some aluminum atoms and to place further aluminum atoms in 4(*c*), and refinement of this second model yielded an *R* value of 8·3%. Neither of these models has fully occupied positions and the corresponding occupancy figures for both models are listed in Table 6. It is difficult to distinguish unambiguously between both models; however, in general the second set affords fewer difficulties in understanding the structure. Also looking at the data one observes that for (101) we observe $F=$zero; for the first model we calculate a rather high value [$F(101)_{calc}=23$], while for the second model $F(101)_{calc}$ is very small. We therefore offer the second model as the correct structure, where we have four boron and

1·8 aluminum atoms in 8(*f*) forming bridges between three icosahedra ending at B(2), B(3), B(3′). In 4(*c*) we find only about 19% of the sites occupied by aluminum.

Table 6. *Statistical distribution of atoms in inter-icosahedral sites for models one and two*

In model one 1·3 electrons per icosahedron are assumed to be transferred from boron atoms in 4(*c*), and 0·7 electrons from aluminum in 8(*f*). In model two no such differentiation is possible. Model two is considered to represent the correct distribution of boron and aluminum.

	Model one		Model two	
Position	Atom	Occupancy figure	Atom	Occupancy figure
8(*f*)	Al	2·7	B(*b*)	4·0
			Al(*b*)	1·79
4(*c*)	B	2·67	Al(1)	0·74
4(*b*)	Al	1·0	Al(2)	1·06
16(*h*)	Al	1·11	Al(3)	1·06
8(*f*)			Al(4)	0·15
Total number of atoms per unit cell:				
Boron		2·7		4·0
Aluminum		4·78		4·8

Of the 5·2 aluminum atoms per unit cell we find a total of 4·8 atoms distributed statistically over five crystallographic sites. The positions were taken from difference Fourier maps during the structure analysis. In 16(*h*) only 6·6% of the sites are occupied; refinement without Al(3), however, stopped at an *R* value of 16·0%, against 8·3% with Al(3) included. The second 8(*f*)′ position, Al(4), with only about 2% occupied, showed up in the last difference Fourier map. Al(4) did not lower *R* much further (from 8·3 to 7·9%) and very likely is of no significance for the structure. It is interesting however to note the hole in the structure with distances of 1·85 and 1·89 Å to B(1) and B(5) respectively, where atoms can easily be placed in isomorphous compounds. Some Al–Al distances (Table 4) appear rather short, and would ask for di- or tri-valent aluminum. Since the sites are, however, only occasionally occupied it is reasonable to conclude that the un-ionized aluminum occupies these sites without hindrance. This is corroborated also by the B–Al distances with a minimum value of 1·96 Å [excluding Al(4)] and an average value of 2·01 Å. The closeness of the positions forces statistical distribution of the aluminum atoms and may offer an explanation for the unreasonable number of 5·2 aluminum atoms. 8(*f*), which is occupied to 72% by boron and aluminum, has one Al(3) neighbour at 1·47 Å and two Al(2) neighbours at 1·74 Å, and there can be atoms at these sites only if 8(*f*) is unoccupied. From Table 6 we find indeed Al(2) and Al(3) occupied to respectively 26·4% and 6·6%. The close packed arrangement of the boron icosahedra leaves holes in the structure, which are, however, too close to each other to be filled completely

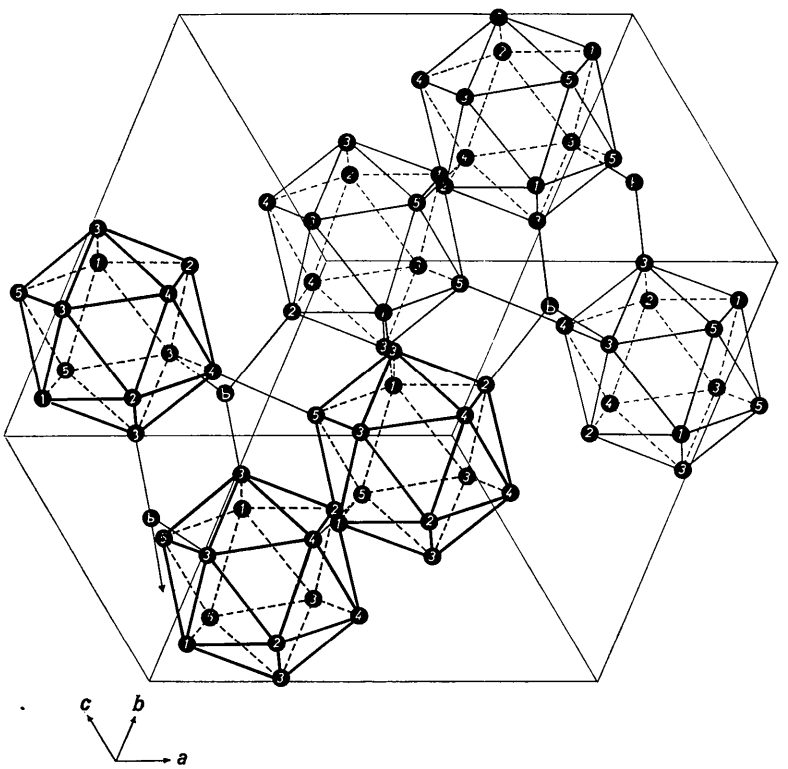

Fig. 7. Diagram of the structure of AlB_{10}

by boron and aluminum atoms. The structure offers a good chance for substitution of aluminum [and the boron atoms in 8(*f*)] by other ions or atoms over a wide range.

The two-dimensional analysis was performed while the author was a staff member of the U.S. Army Electronics Research and Development Laboratory, Fort Monmouth, New Jersey, U.S.A. It is a pleasure to acknowledge the continuing interest and many profitable discussions during that time with Dr J. A. Kohn, who also kindly provided the crystal. The three-dimensional work was done at the Eduard Zintl Institut, Technische Hochschule, Darmstadt, and it is my special privilege to thank Prof. Wölfel for his interest and encouragement. I am further indebted to Mrs H. Gross for the densitometer measurements, and the Deutsches Rechenzentrum and the Rechenzentrum der Technischen Hochschule Darmstadt for providing computer time.

References

CLARK, H. K. & HOARD, J. L. (1943). *J. Amer. Chem. Soc.* **65**, 2115.
DECKER, B. F. & KASPER, J. S. (1959). *Acta Cryst.* **12**, 503.
ERIKS, C. (1961). Private communication.
HOARD, J. L., HUGHES, R. E. & SANDS, D. E. (1958). *J. Amer. Chem. Soc.* **80**, 4507.
HOPPE, W. (1957). *Z. Elektrochem.* **61**, 1076.
HOPPE, W. & WILL, G. (1960). *Z. Kristallogr.* **113**, 104.
HUGHES, R. E., KENNARD, C. H. L., SULLENGER, D. B., WEAKLIEM, H. A., SANDS, D. E. & HOARD, J. L. (1963). *J. Amer. Chem. Soc.* **85**, 361.
KOHN, J. A., KATZ, G. & GIARDINI, A. A. (1958). *Z. Kristallogr.* **111**, 53.
LIPSCOMB, W. N. & BRITTON, D. (1960). *J. Chem. Phys.* **33**, 275.
LONGUET-HIGGINS, H. C. & ROBERTS, M. DE V. (1955). *Proc. Roy. Soc.* A, **230**, 110.
WILL, G. (1963*a*). *Z. Kristallogr.* **119**, 1.
WILL, G. (1963*b*). *J. Amer. Chem. Soc.* **85**, 2335.
WILL, G. (1964). USAELRDL Technical Report 2436.

Acta Cryst. (1967). **23**, 1079

The Crystal Structure of Dimanganese Iron Carbonyl, $Mn_2Fe(CO)_{14}$*

BY P. A. AGRON, R. D. ELLISON AND H. A. LEVY

Chemistry Division, Oak Ridge National Laboratory, Oak Ridge, Tennessee, U.S.A.

(*Received* 28 *April* 1967)

X-ray peak-top data were collected with a computer-controlled diffractometer programmed to optimize precision by adjusting peak and background counting times and to reject weak reflections. The structure was solved by inspection of the Patterson diagram. The structure contains two crystallographically distinct molecules of symmetry 2/*m*. The iron atoms are situated at the non-equivalent symmetry centers 000 and $0\frac{1}{2}\frac{1}{2}$ of the monoclinic unit cell ($C2/m$, $a=11{\cdot}94$, $b=14{\cdot}29$, $c=11{\cdot}73$ Å, $\beta=97{\cdot}23°$, $Z=4$). Both molecules have linear arrangements of metal atoms, without bridging carbonyl linkages. Each metal atom is essentially octahedral, with the carbonyl ligands on Mn oriented at 45° to those on Fe. The molecules differ in disposition of symmetry elements: in one, three metal atoms, two carbonyl ligands of Fe, and the apical ligands of Mn lie in the mirror, with the remaining ligands of Fe along the diad; in the other, the metal atoms and the apical ligands lie along the diad, with the remaining 4 ligands of Fe in the mirror. Interatomic distances are Fe–Mn, 2·80–2·83; Fe–C, 1·79–1·80; Mn–C (apical), 1·80–1·82; Mn–C (equatorial), 1·85–1·86; C–O, 1·12–1·15 Å.

Bonding between the metal atoms in polynuclear metal carbonyls is of two kinds. In some compounds the carbonyl group forms a bridge, as in $Fe_2(CO)_9$ (Powell & Ewens, 1939); in other cases the metal atoms are directly linked, as in $Mn_2(CO)_{10}$ (Dahl & Rundle, 1963; Bailey & Dahl, 1965) and its rhenium and technetium analogues. Compounds with bridging carbonyl groups show a characteristic infrared absorption band at about 1850 cm^{-1}.

A trinuclear carbonyl identified as $Mn_2Fe(CO)_{14}$ has been prepared by Schubert & Sheline (1965) by the photolysis with ultraviolet light of an equimolar solution of $Fe(CO)_5$ and $Mn_2(CO)_{10}$ in n-hexane. In the spectrum of this compound there is no band in the neighborhood of 1850 cm^{-1} (private communication); thus it appeared likely that the molecule had the structure $(CO)_5MnFe(CO)_4Mn(CO)_5$ without bridging CO groups. The present study confirms this hypothesis and establishes the molecular configuration and dimensions.

Experimental

A sample of the red, needle-shaped crystals was furnished by Professor Sheline and Dr George Evans of Florida State University. The specimen selected for

* Research sponsored by the U.S. Atomic Energy Commission under contract with the Union Carbide Corporation.